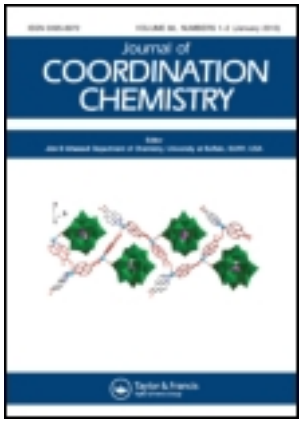

Journal of Coordination Chemistry
Publication details, including instructions for authors and subscription information:
http://www.tandfonline.com/loi/gcoo20

Hydrothermal synthesis and structural characterization of three reduced phosphomolybdates

Xiao Xu [a], Weiwei Ju [a], Dawei Yan [b], Ningge Jian [a] & Yan Xu [a]
[a] State Key Laboratory of Materials-oriented Chemical Engineering, College of Chemistry and Chemical Engineering, Nanjing University of Technology, Nanjing, P.R. China
[b] Jiangsu Engineering Technology Research Center for Energy Conservation and Emission Reduction of Transportation, Nanjing Communication Institute of Technology, Nanjing, P.R. China
Accepted author version posted online: 04 Jun 2013.Published online: 16 Jul 2013.

To cite this article: Xiao Xu, Weiwei Ju, Dawei Yan, Ningge Jian & Yan Xu (2013) Hydrothermal synthesis and structural characterization of three reduced phosphomolybdates, Journal of Coordination Chemistry, 66:15, 2669-2678, DOI: 10.1080/00958972.2013.811498

To link to this article: http://dx.doi.org/10.1080/00958972.2013.811498

Journal of Coordination Chemistry, 2013
Vol. 66, No. 15, 2669–2678, http://dx.doi.org/10.1080/00958972.2013.811498

Hydrothermal synthesis and structural characterization of three reduced phosphomolybdates

XIAO XU†, WEIWEI JU†, DAWEI YAN‡, NINGGE JIAN† and YAN XU*†

†State Key Laboratory of Materials-oriented Chemical Engineering, College of Chemistry and Chemical Engineering, Nanjing University of Technology, Nanjing, P.R. China
‡Jiangsu Engineering Technology Research Center for Energy Conservation and Emission Reduction of Transportation, Nanjing Communication Institute of Technology, Nanjing, P.R. China

(*Received 5 February 2013; in final form 18 April 2013*)

Three reduced molybdenum(V) phosphates, $Na_2[H_2DaHex]_{4.5}[H_3O]\{Mn[Mo_6O_{12}(OH)_3(HPO_4)_2(PO_4)_2]_2\}\cdot 2H_2O$ (**1**), $[H_2DaHex]_4[Zn(H_2O)]_2\{Zn[Mo_6O_{12}(OH)_3(HPO_4)_2(PO_4)_2]_2\}\cdot 6H_2O$ (**2**), and $[H_2DaHex]_{3.5}[Cd(H_2O)_2]_{1.5}[Cd(H_2O)]\{Cd[Mo_6O_{12}(OH)_3(HPO_4)_2(PO_4)_2]_2\}\cdot 3.5H_2O$ (**3**) (DaHex = 1,6-diaminylhexane), were hydrothermally synthesized by using the same organic template (DaHex) and characterized by elemental analysis, IR, TGA, powder XRD, and single-crystal X-ray diffraction. Crystallographic analysis reveals that the compounds contain $M[P_4Mo_6]_2$ (M = Mn for **1**, Zn for **2**, Cd for **3**) polyanions, which are further connected by various metal ions to form different topological structures. In **1**, the cluster anion $Mn[P_4Mo_6]_2$ is discrete. For **2** and **3**, $M[P_4Mo_6]_2$ (Zn for **2**, Cd for **3**) clusters are linked by transition metal ions to form different infinite chains. Then, all the 1-D chains are further packed into 3-D supramolecular structures via hydrogen-bonding interactions. The formations of **1**, **2,** and **3** demonstrate that not only organic templates, but transition metal ions also play very important roles in the M-P_4Mo_6 system.

Keywords: Hydrothermal synthesis; Phosphomolybdates; Crystal structure; 1-D chain

1. Introduction

Polyoxometalates (POMs) have many properties that make them attractive for applications in catalysis, biology, magnetism, materials science, optics, and medicine [1–8]. As a branch of POMs, phosphomolybdates have attracted attention since they were solvothermally synthesized and structurally characterized [9–12]. Recently, to construct high dimensional compounds with unique topologies and properties, transition metals were introduced to the synthesis of phosphomolybdates. In these compounds, transition metals not only act as counter ions but also as bridging ions which link phosphomolybdates via covalent bonds [13]. A series of hybrid transition metal molybdenum phosphates have been obtained [14–23]. Organic amines play important roles in the synthesis of POM-based hybrid materials. In general, organic amines are regarded as structure-directing agents, controlling the structure of polyoxometalates. The assembly of these POMs in the presence of

*Corresponding author. Email: yanxu@njut.edu.cn

structure-directing protonated organic amines can form porous frameworks with layered or channel-like structures [24]. Organic amines also can act as reducing agents in the reaction system of reduced phosphomolybdates. As charge-compensating cations, they can balance the charge of the system.

In our previous work, reduced phosphomolybdates based on ethylenediamine and 1,2-diaminopropane have been investigated to show the influence of organic amines on the structure of the products [25, 26]. As a continuation, here we report three new compounds based on 1,6-diaminylhexane and reduced phosphomolybdates, formulated as, $Na_2[H_2DaHex]_{4.5}[H_3O]\{Mn[Mo_6O_{12}(OH)_3(HPO_4)_2(PO_4)_2]_2\}\cdot 2H_2O$ (**1**), $[H_2DaHex]_4[Zn(H_2O)]_2\{Zn[Mo_6O_{12}(OH)_3(HPO_4)_2(PO_4)_2]_2\}\cdot 6H_2O$ (**2**), and $[H_2DaHex]_{3.5}[Cd(H_2O)_2]_{1.5}[Cd(H_2O)]\{Cd[Mo_6O_{12}(OH)_3(HPO_4)_2(PO_4)_2]_2\}\cdot 3.5H_2O$ (**3**). Although three new reduced molybdenum (V) phosphates, **1**, **2,** and **3** were synthesized by using the same organic template (DaHex), their topological structures are very different. The structural analysis of **1**, **2,** and **3** indicate that not only organic templates, but also transition metal ions play very important roles in M-P_4Mo_6.

2. Experimental

2.1. *Materials and equipment*

All chemicals purchased were of reagent grade and used without purification. Elemental analyses (C, H, N) were performed on a Perkin-Elmer 2400 elemental analyzer. IR spectra of **1–3** were recorded with a Nicolet Impact 410 FTIR spectrometer with pressed KBr pellets from 4000–500 cm^{-1}. TG measurement was carried out on a Diamond thermogravimetric analyzer in flowing N_2 from 50 to 800 °C with a heating rate of 10 °C·min^{-1}. Powder X-ray diffraction (PXRD) data were obtained using a Bruker D8 Advance diffractometer with Cu K_α radiation ($\lambda = 1.54056$ Å), with a step speed of 0.1° per second.

2.2. *Syntheses of the complexes*

2.2.1. $Na_2[H_2DaHex]_{4.5}[H_3O]\{Mn[Mo_6O_{12}(OH)_3(HPO_4)_2(PO_4)_2]_2\}\cdot 2H_2O$ (1). A mixture of Na_2MoO_4 (2.0706 g), manganese acetate (1.0488 g), 1,6-diaminylhexane (3.0418 g), and deionized water (6 mL) was stirred for 20 min in open air and when 50% H_3PO_4 was added to the mixture; the final pH was 4. Then the solution was stirred for another 20 min. At last the mixture was transferred to a 20 mL Teflon-lined autoclave and heated to 160 °C for seven days. After cooling to room temperature, reddish block-like crystals were filtered, washed with deionized water, and dried in air (0.2682 g, yield 32% based on Mo). Elemental analysis found: C 10.16%, H 3.37%, and N 4.18% (Calcd C 10.34%, H 3.29%, and N 4.02%).

2.2.2. $[H_2DaHex]_4[Zn(H_2O)]_2\{Zn[Mo_6O_{12}(OH)_3(HPO_4)_2(PO_4)_2]_2\}\cdot 6H_2O$ (2). A mixture of MoO_3 (0.1533 g), cadmium acetate (0.1413 g), 1,6-diaminylhexane (0.5060 g), and deionized water (8 mL) was stirred for 20 min in open air and 50% H_3PO_4 was added to the mixture; the final pH was 4. Then the solution was stirred for another 20 min. At last the mixture was transferred to a 20 mL Teflon-lined autoclave and heated to 160 °C for

seven days. After being cooled to room temperature, brown block-like crystals were filtered, washed with deionized water, and dried in air (0.2374 g, yield 28% based on Mo). Elemental analysis found: C 7.49%, H 2.60%, and N 3.01% (Calcd C 7.54%, H 2.63%, and N 2.93%).

2.2.3. $[H_2DaHex]_{3.5}[Cd(H_2O)_2]_{1.5}[Cd(H_2O)]\{Cd[Mo_6O_{12}(OH)_3(HPO_4)_2(PO_4)_2]_2\}\cdot 3.5H_2O$ (3). A mixture of MoO_3 (0.61 g), zinc acetate (0.4638 g), 1,6-diaminylhexane (0.9900 g), and deionized water (8 mL) was stirred for 20 min in open air and 50% H_3PO_4 was added to the mixture; the final pH was 4. Then, the solution was stirred for another 20 min. At last, the mixture was transferred to a 20 mL Teflon-lined autoclave and heated to 160 °C for seven days. After cooling to room temperature, brown block-like crystals were filtered, washed with deionized water and dried in air (0.2625 g, yield 23% based on Mo). Elemental analysis found: C 9.02%, H 3.12%, and N 3.40% (Calcd C 8.96%, H 3.05%, and N 3.48%).

2.3. *X-ray crystallography*

Single crystals of **1–3** were selected by visual examination under the microscope and glued at the top of a thin glass fiber with epoxy glue in air for data collection; the crystallographic data were collected on a Bruker Apex II CCD with Mo-K_α radiation ($\lambda = 0.71073$ Å) at 296 K using ω-2θ scan method. The crystal structures were solved by direct methods and refined on $|F|^2$ by full-matrix least-squares using SHELX97 [27]. All non-hydrogen atoms were refined anisotropically. Hydrogens of organic amines for complexes were placed in calculated positions. Hydrogens of water and OH groups were not located. Some disordered waters had partial occupation. The crystal data are presented in table 1.

3. Results and discussion

3.1. *Synthesis*

Many factors, such as pH, reaction time, organic amines, and transition metals, can influence the final crystal structures. Organic amines play crucial roles on the supramolecular structure of the POM framework. Equivalent reactions indicate that no crystals could be obtained without 1,6-diaminylhexane. Usually, rigid amines induced the formation of layered arrangements, whereas structurally more flexible amines resulted in formation of polymeric chains [28]. In this paper, we focus on the influence of pH and transition metals. We obtained three different compounds by using the same organic amine template (DaHex) at pH 4. If the pH was lower than 4 or higher than 4, no crystals could be obtained. Transition metals play an important role during synthesis of M-$[P_4Mo_6]_2$. In **1**, the cluster anion $Mn[P_4Mo_6]_2$ is discrete. For **2** and **3**, $M[P_4Mo_6]_2$ (Zn for **2**, Cd for **3**) clusters are linked by transition metal ions to form different infinite chains.

3.2. *Crystal structure*

The dimeric polyoxomolybdenum(V) phosphate anion $M[P_4Mo_6]_2$ (M=Mn for **1**, Zn for **2**, Cd for **3**) appears in the structure of **1–3** (figure 1(b)). The classical sandwich-type anion is based on two planar hexanuclear $\{Mo_6\}$ rings (figure 1(a)), each formed by six

Table 1. Crystal data and structure refinement for **1–3**.

Compound	**1**	**2**	**3**
Empirical formula	$Na_2C_{27}H_{89}N_{6.5}O_{67.5}P_8Mo_{12}Mn$	$C_{24}H_{88}Mo_{12}N_8O_{70}P_8Zn_3$	$C_{21}H_{88}Cd_{3.5}Mo_{12}N_7O_{69.5}P_8$
Formula weight	3085.01	3204.17	3343.42
Temperature (K)	296(2)	296(2)	296(2)
Wavelength (A)	0.71073	0.71073	0.71073
Crystal system	Monoclinic	Triclinic	Triclinic
Space group	$P2/c$	$P\bar{1}$	$P\bar{1}$
Unit cell dimensions (Å, °)			
a	27.3088(19)	12.0198(8)	11.9935(6)
b	12.0013(8)	13.8168(9)	16.9747(8)
c	27.2755(19)	13.9586(9)	20.7213(10)
α	90	72.256(1)	92.052(1)
β	108.372(1)	75.339(1)	98.130(1)
γ	90	80.307(1)	91.617(1)
Volume ($Å^3$)	8483.7(10)	2125.5(2)	4171.1(4)
Z	4	1	2
Calculated density ($g\,cm^{-3}$)	2.415	2.503	2.662
Absorption coefficient	2.132	2.805	2.882
F (0 0 0)	6030	1562	3222
Crystal size	$0.16 \times 0.14 \times 0.12$	$0.13 \times 0.12 \times 0.11$	$0.18 \times 0.14 \times 0.12$
Limiting indices	$-32 \leqslant h \leqslant 32$ $-14 \leqslant k \leqslant 13$ $-32 \leqslant l \leqslant 32$	$-14 \leqslant h \leqslant 14$ $-16 \leqslant k \leqslant 16$ $-15 \leqslant l \leqslant 16$	$-13 \leqslant h \leqslant 14$ $-20 \leqslant k \leqslant 20$ $-24 \leqslant l \leqslant 24$
Reflections collected/ unique	59,176/14,992 [R(int) = 0.0738]	15,100/7431 [R(int) = 0.0172]	29,939/14,549 [R(int) = 0.0328]
Max. and min. transmission	0.7840 and 0.7266	0.7478 and 0.7119	0.7236 and 0.6250
Data/parameters	14,992/1177	7432/602	14,549/1163
Goodness-of-fit on $\|F\|^2$	1.065	1.148	1.163
Final R indices [$I > 2\sigma(I)$]	$R_1 = 0.0423$, $wR_2 = 0.1132$	$R_1 = 0.0237$, $wR_2 = 0.0742$	$R_1 = 0.0407$, $wR_2 = 0.1031$
	$R_1 = 0.0583$, $wR_2 = 0.1252$	$R_1 = 0.0275$, $wR_2 = 0.0853$	$R_1 = 0.0610$, $wR_2 = 0.1117$

edge-sharing MoO_6 octahedra with alternating bonding (average 2.584 Å for **1**, 2.595 Å for **2** and 2.610 Å for **3**) and non-bonding Mo–Mo distances (average 3.499 Å for **1**, 3.508 Å for **2** and 3.561 Å for **3**). The Mo–O distances are 1.674(4)–2.315(4) Å for **1**, 1.676(3)–2.304(3) Å for **2,** and 1.666(3)–2.361(3) Å for **3**, respectively. The O–Mo–O angles are between 72.03(14)–171.59(18)° for **1**, 73.06(10)–170.47(12)° for **2,** and 69.75(12)–170.22 (14)° for **3**. In the outer $\{Mo_6\}$ ring, three peripheral and one central PO_4 tetrahedra are located on the same side of the ring plane. The central PO_4 tetrahedron and three other peripheral PO_4 groups bridge the non-bonding Mo–Mo fragments and further reinforce the structure. The P–O distances vary from 1.465(5) to 1.581(5) Å for **1**, 1.511(3)–1.552(3) Å for **2,** and 1.503(4)–1.573(4) Å for **3** and the O–P–O angles are between 104.8(3) and 115.3(2)° for **1**, 104.13(17) and 114.11(19)° for **2** and 105.44(19) and 114.5(2)° for **3**. All the bond lengths and angles are in agreement with reported compounds [29–34]. The assignment of oxidation states of Mo for **1–3** are based on bond valence sum calculations [35], which gives the average value 4.86 for **1**, 4.83 for **2,** and 4.92 for **3** Mo^{VI} can be reduced to Mo^{V} in the presence of organic amines under hydrothermal conditions and the calculation results confirm that Mo has the oxidation state of + 5 in **1–3**.

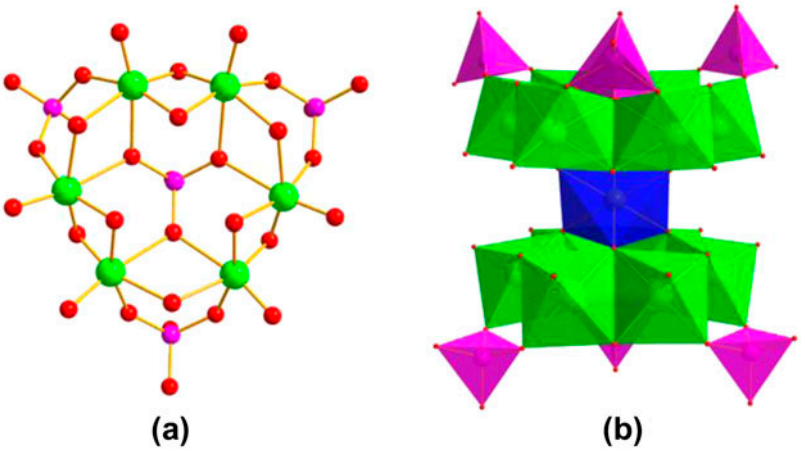

Figure 1. (a) The $[P_4Mo_6]$ unit. (b) The dimeric anion $M[P_4Mo_6]_2$ (M=Mn for **1**, Zn for **2**, Cd for **3**).

The asymmetric unit of $Na_2[H_2DaHex]_{4.5}[H_3O]\{Mn[Mo_6O_{12}(OH)_3(HPO_4)_2(PO_4)_2]_2\}\cdot 2H_2O$ (**1**) consists of one manganese ion, two sodium ions, two $[P_4Mo_6]$ units, four and one half protonated 1,6-diaminylhexanes, and three lattice waters. O(19) and O(60) with longer P–O bonds [P(1)–O(19), 1.565(4) Å; P(5)–O(60), 1.581(5) Å] and μ_2–O [O(11), O(22), O(17)] between two adjacent Mo ions can be ascribed to OH^- groups due to their bond valence sum values of 1.096–1.114. Thus, the anion can be formulated as $[Mo_6O_{12}(OH)_3(HPO_4)_2(PO_4)_2]^{7-}$. In the structure of **1**, there exists only one coordination type of Mn, which bridges two $[P_4Mo_6]$ clusters by six μ_3–O to form a classical sandwich-type anion; the distances of Mn–O are 2.189(4)–2.236(4) Å. The discrete cluster anions $\{Mn[Mo_6O_{12}(OH)_3(HPO_4)_2(PO_4)_2]_2\}^{12-}$ were connected by electrostatic interaction of Na^+ to form an infinite chain. The interchain spaces of **1** between adjacent chains are occupied by protonated 1,6-diaminylhexane, as counter ions and stabilizing the structure (figure 2).

Crystal structure analysis reveals that the asymmetric unit of $[H_2DaHex]_4[Zn(H_2O)]_2\{Zn[Mo_6O_{12}(OH)_3(HPO_4)_2(PO_4)_2]_2\}\cdot 6H_2O$ (**2**) is made up of two Zn ions, one $[P_4Mo_6]$ polyoxoanion, two protonated 1,6-diaminlyhexanes, and three lattice waters. Some P–O bonds

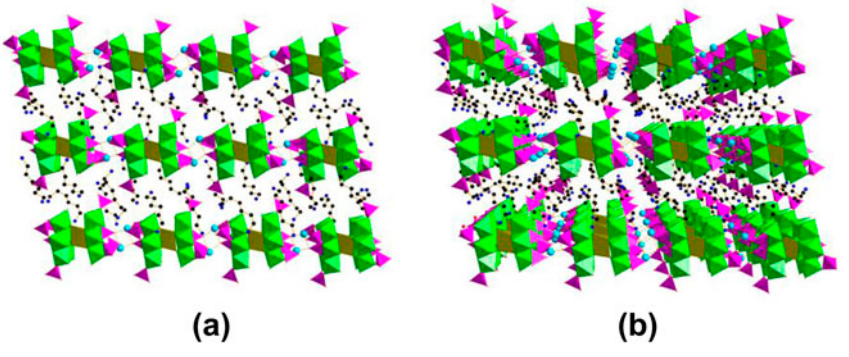

Figure 2. (a) The 2-D supermolecular sheet of **1** along the *b* axis. (b) The 3-D supermolecular framework of **1**. Waters and hydrogens are omitted for clarity.

[P(3)–O(28), 1.571(3); P(2)–O(29), 1.552(3)] are longer than other P–O groups. The μ_2–O [O(13), O(6), O(8)] between adjacent Mo atoms, O(28) and O(29) can be ascribed to OH^- groups due to their bond valence sum values of 1.126–1.185 Å. Thus, the anion can be formulated as $[Mo_6O_{12}(OH)_3(HPO_4)_2(PO_4)_2]^{7-}$. In **2**, Zn has two coordination types. Zn (1) is octahedral, coordinated by six μ_3–O from adjacent $[P_4Mo_6]$ units to form a classical sandwich-type anion, $\{Zn[Mo_6O_{12}(OH)_3(HPO_4)_2(PO_4)_2]_2\}^{12-}$, with Zn–O bond distance of 2.143(2)–2.188(3) Å. Zn(2) shows tetrahedral geometry, coordinated by one coordination water and three μ_2–O from adjacent $[P_4Mo_6]$ units, with Zn–O bond distances of 1.911(3)–2.008(3) Å. The sandwich-shaped $Zn[P_4Mo_6]_2$ anions, as the basic building units are linked by Zn(2) to form an infinite $[Zn(H_2O)]_2\{Zn[Mo_6O_{12}(OH)_3(HPO_4)_2(PO_4)_2]_2\}_n^{8n-}$ chain (figure 3). Protonated 1,6-diaminylhexane fills into adjacent chains and each chain is linked by 1,6-diaminylhexanes through hydrogen bonds (N–H···O) to generate a layer, exhibited in figure 4(a). Adjacent layers are also connected through hydrogen bonds to form a 3-D supermolecular structure (figure 4b).

When we use cadmium acetate to replace zinc acetate, $[H_2DaHex]_{3.5}[Cd(H_2O)_2]_{1.5}[Cd(H_2O)]\{Cd[Mo_6O_{12}(OH)_3(HPO_4)_2(PO_4)_2]_2\}\cdot 3.5H_2O$ (**3**) was obtained. The asymmetric unit of **3** consists of four Cd^{2+} ions, two $[P_4Mo_6]$ polyoxoanions, three and one-half protonated 1,6-diaminylhexanes, and four lattice waters. Terminal O(56) and O(61) with longer P–O bonds [P(3)–O(56), 1.558(3) Å; P(1)–O(61), 1.573(4) Å] and μ_2–O [O(6), O(18), O(21)] between two adjacent Mo ions can be ascribed to OH^- groups due to their bond valence sum values of 1.120–1.167. Thus, the anion can be formulated as $[Mo_6O_{12}(OH)_3(HPO_4)_2(PO_4)_2]^{7-}$. There are four crystallographically different Cd ions, which exhibit four coordination environments in **3**. Cd(1) exhibits a distorted octahedral geometry, coordinated by six μ_3–O from adjacent $[P_4Mo_6]$ units to form a classical sandwich-type anion, $\{Cd[Mo_6O_{12}(OH)_3(HPO_4)_2(PO_4)_2]_2\}^{12-}$; the distances of Cd(1)–O are 2.255(3)–2.313(3) Å. Cd(2) is six-coordinate by two coordinated waters and four O from adjacent sandwich-type polyoxoanions, with Cd(2)–O bond distance of 2.225(3)–2.351(5) Å. Cd(3)

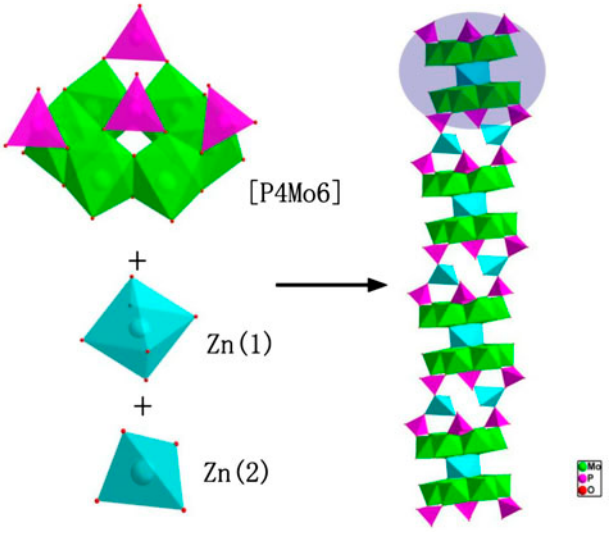

Figure 3. The schematic representation of the formation of the infinite chain based on $[P_4Mo_6]$ and Zn^{2+} in **2**. The blue shadow means the sandwich-type polyoxoanion (see http://dx.doi.org/10.1080/00958972.2013.811498 for color version).

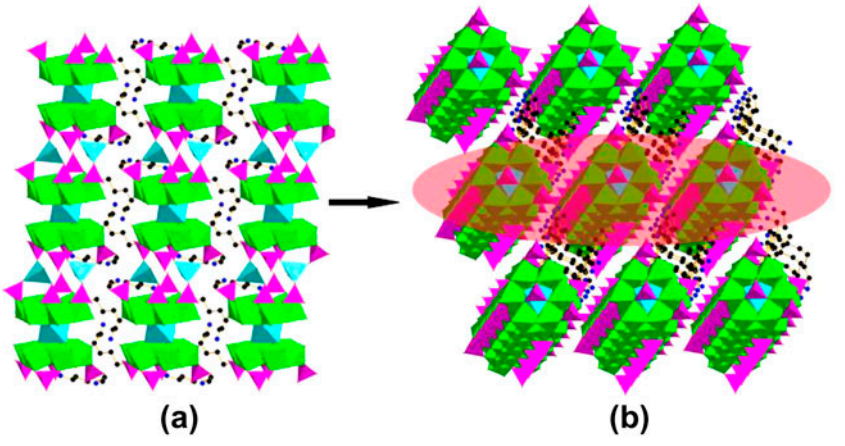

Figure 4. (a) The 2-D layer of **2** via intermolecular hydrogen bonds. (b) The 3-D supermolecular structure of **2**. Waters and hydrogens are omitted for clarity.

is seven-coordinate by two coordinated waters and five O from adjacent sandwich-type polyoxoanions to form a distorted decahedral geometry, with Cd(3)–O bond distance of 2.214(3)–2.376(4) Å. Cd(4) is five coordinate by one coordinated water and four O to form a rectangular pyramid geometry, with Cd(4)–O bond distance of 2.139(3)–2.438(3) Å. In **3**, two Cd(4) link to form a binuclear Cd–O cluster through sharing the μ_3–O. One Cd(2) and two Cd(3) form a trinuclear Cd–O cluster. Neighboring $Cd[P_4Mo_6]_2$ are connected by binuclear Cd–O cluster and trinuclear Cd–O cluster alternately to form an infinite $[Cd(H_2O)_2]_{1.5}[Cd(H_2O)]\{Cd[Mo_6O_{12}(OH)_3(HPO_4)_2(PO_4)_2]_2\}_n^{7n-}$ chain (figure 5). In the lattice, the polymeric chains are arranged parallel. Spaces between chains are filled with protonated 1,6-diaminylhexane cations. Further, these organic amines stabilize the framework by both electrostatic and hydrogen bonding interactions (figure 6).

3.3. *Infrared spectra*

IR spectra of **1–3** exhibit similar characteristic peaks (figures S1–S3). Peaks at 606–744 cm^{-1} are attributed to ν(Mo–O–Mo) vibrations. Strong peaks at 956–966 cm^{-1} are due to ν(Mo=O) vibrations. The ν(P–O) ranges from 1033–1178 cm^{-1}. Strong peaks at 1384–1622 cm^{-1} are assigned to C–C and C–N stretch of organic amines. In addition, broad bands at 3247–3440 cm^{-1} are due to ν(O–H) and ν(N–H). The features are in agreement with reported compounds [22, 35, 36].

3.4. *TG analysis*

The TG curve of **1** indicates that weight loss can be divided into two distinct stages (figure S4, black). The first weight loss of 4.62% (Calcd 4.43%) at 50–250 °C corresponds to loss of water. From 250 to 800 °C, the second weight loss is attributed to decomposition of 1,6-diaminylhexane (weight loss: exp. 21.98%, Calcd 21.21%).

The TG curve of **2** indicates that weight loss can be divided into two distinct stages (figure S4, red). The first weight loss of 4.12% (Calcd 4.56%) at 50–250 °C corresponds to

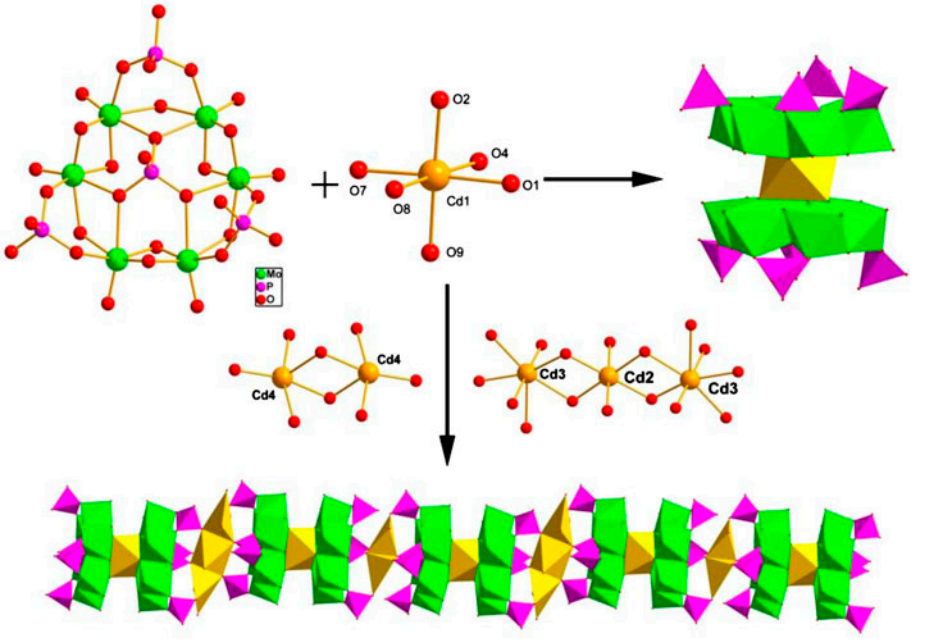

Figure 5. The schematic representation of the formation of the infinite chain based on $[P_4Mo_6]$ and Cd^{2+} in **3**.

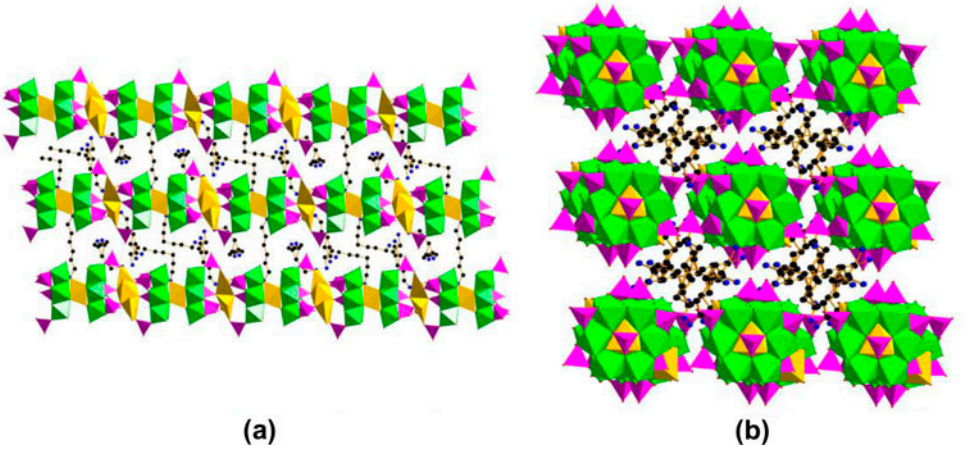

Figure 6. (a) The 2-D layer of **3** via intermolecular hydrogen bond interactions. (b) The 3-D supermolecular structure of **3**. Waters and hydrogens are omitted for clarity.

loss of water. From 250 to 700 °C, the second weight loss is attributed to decomposition of 1,6-diaminylhexane (weight loss: exp. 22.93%, Calcd 22.32%).

The TG curve of **3** shows two steps of weight loss (figure S6). The first of 3.12% (Calcd 3.28%) at 50–300 °C corresponds to loss of water. From 300 to 800 °C, the second weight loss is attributed to decomposition of 1,6-diaminylhexane (weight loss: exp. 19.88%, Calcd 17.38%).

3.5. *Powder X-ray diffractions*

Figures S5–S7 present the PXRD patterns for **1–3**. The diffraction peaks of both simulated and experimental patterns match well in relevant positions, thus indicating that the phase purities of **1–3** are good. The difference in reflection intensities between the simulated and the experimental patterns is due to different orientation of the crystals in the powder samples.

4. Conclusions

Three new compounds based on reduced phosphomolybdates were synthesized under hydrothermal conditions by using the same organic amine. Compound **1** contains discrete $Mn[P_4Mo_6]_2$ units. For **2**, the organic amines form infinite $[Zn(H_2O)]_2\{Zn[Mo_6O_{12}(OH)_3(HPO_4)_2(PO_4)_2]_2\}_n^{8n-}$ chains constructed from Zn^{2+} and $Zn[P_4Mo_6]_2$. In **3**, neighboring $Cd[P_4Mo_6]_2$ was connected by binuclear Cd–O moiety and trinuclear Cd–O moiety alternately to form 1-D $[Cd(H_2O)_2]_{1.5}[Cd(H_2O)]\{Cd[Mo_6O_{12}(OH)_3(HPO_4)_2(PO_4)_2]_2\}_n^{7n-}$ chains. In previous, we obtained two reduced phosphomolybdates by using ethylenediamine and 1,2-diaminopropane as structure-directing reagents; different organic amines template diverse formation of POMs-based compounds. In this work, formation of the three compounds reveals that not only organic amines, but also transition metals play an important role during the synthesis for M-$[P_4Mo_6]_2$.

Supplementary material

CCDC-922341, 922342, and 922343 contain the supplementary crystallographic data for **1**, **2,** and **3**. These data can be obtained free of charge via http://www.ccdc.cam.ac.uk/conts/retrieving.html, or from Cambridge Crystallographic Data Center, 12 Union Road, Cambridge CB2 1E2, UK; Fax: (+44) 1223-336-033; or E-mail: deposit@ccdc.cam.ac.uk.

Acknowledgment

We thank the National Natural Science Foundation of China (20971068) and Jiangsu Province (Grant BK2012823) for financial support.

References

[1] C.L. Hill. *Chem. Rev.*, **98**, 1 (1998).
[2] D.E. Katsoulis. *Chem. Rev.*, **98**, 359 (1988).
[3] H.C. Liu, N. Bayat, E. Iglesia. *Angew. Chem. Int. Ed.*, **42**, 5072 (2003).
[4] J.M. Poblet, X. López, C. Bo. *Chem. Soc. Rev.*, **32**, 297 (2003).
[5] M. Sadakane, E. Steckhan. *Chem. Rev.*, **98**, 219 (1998).
[6] A.K. Cheetham, G. Ferey, T. Loiseau. *Angew. Chem. Int. Ed.*, **38**, 3268 (1999).
[7] J.M. Clemente-Juan, E. Coronado, A. Gaita-Arino. *Chem. Soc. Rev.*, **41**, 7464 (2012).
[8] S. Cardona-Serra, J.M. Clemente-Juan, E. Coronado, A. Gaita-Arino, A. Camon, M. Evangelisti, F. Luis, M.J. Martinez-Perez, J. Sese. *J. Am. Chem. Soc.*, **134**, 14982 (2012).
[9] X.L. Wang, C. Qin, E.B. Wang, Z.M. Su, Y.G. Li, L. Xu. *Angew. Chem. Int. Ed.*, **45**, 7411 (2006).

[10] T. Akutagawa, D. Endo, S.I. Noro, L. Cronin, T. Nakamura. *Coord. Chem. Rev.*, **251**, 2547 (2007).
[11] D.L. Long, R. Tsunashima, L. Cronin. *Angew. Chem. Int. Ed.*, **49**, 1736 (2010).
[12] A. Proust, R. Thouvenot, P. Gouzerh. *Chem. Commun.*, **1837**, (2008).
[13] Y. Ma, Y.G. Li, E.B. Wang, Y. Lu, X.X. Xu. *J. Mol. Struct.*, **791**, 10 (2006).
[14] L.A. Meyer, R.C. Haushalter. *Inorg. Chem.*, **32**, 1579 (1993).
[15] L. Xu, Y.Q. Sun, E.B. Wang, E.H. Shen, Z.R. Liu, C.W. Hu, X. Yan, Y. Lin, H.Q. Jia. *New J. Chem.*, **23**, 1041 (1999).
[16] C.D. Peloux, P. Mialane, A. Dolbecq, J. Marrot, E. Riviereb, F. Secheresse. *J. Mater. Chem.*, **11**, 3392 (2001).
[17] L.Y. Duan, F.C. Liu, X.L. Wang, E.B. Wang, C. Qin, Y.G. Li, C.W. Hu. *J. Mol. Struct.*, **705**, 15 (2004).
[18] H.X. Guo, S.X. Liu. *J. Mol. Struct.*, **751**, 156 (2005).
[19] W.J. Chang, Y.C. Jiang, S.L. Wang, K.H. Li. *Inorg. Chem.*, **45**, 6586 (2007).
[20] Q. Chen, Y. Cui, Q. Sun, W.J. Pan, Y. Xu. *Z. Anorg. Allg. Chem.*, **635**, 2302 (2009).
[21] C. Streb, D.L. Long, L. Cronin. *CrystEngComm*, **8**, 629 (2006).
[22] J. Liu, E.B. Wang, X.L. Wang, D.R. Xiao, L.L. Fan. *J. Mol. Struct.*, **867**, 206 (2008).
[23] X.L. Wang, J. Li, A.X. Tian, D. Zhao, G.C. Liu, H.Y. Lin. *Cryst. Growth Des.*, **11**, 3456 (2011).
[24] Y.N. Zhang, B.B. Zhou, J.Q. Sha, Z.H. Su, J.W. Cui. *J. Solid State Chem.*, **184**, 419 (2011).
[25] D.W. Yan, J. Fu, L. Zheng, Z.B. Zhang, Y. Xu, X.L. Zhu, D.R. Zhu. *CrystEngComm*, **13**, 5133 (2011).
[26] X. Xu, D.W. Yan, X.R. Fan, Y. Xu. *J. Coord. Chem.*, **65**, 3674 (2012).
[27] G.M. Sheldrick. *SHELXTL version 5.10*, Bruker AXS Inc., Madison, WI (1997).
[28] C.P. Pradeep, D.L. Long, L. Cronin. *Dalton Trans.*, **39**, 9443 (2010).
[29] W.B. Yang, C.Z. Lu, C.D. Wu, S.F. Lu, D.M. Wu. *J. Cluster Sci.*, **13**, 43 (2002).
[30] C.D. Peloux, P. Mialane, A. Dolbecq, J. Marrot, E. Riviere, F. Secheresse. *J. Mater. Chem.*, **11**, 3392 (2001).
[31] Y. Ma, Y.G. Li, E.B. Wang, Y. Lu, X.L. Wang, D.R. Xiao, X. Xu. *Inorg. Chim. Acta*, **360**, 421 (2007).
[32] W.J. Chang, Y.C. Jiang, S.L. Wang, K.H. Lii. *Inorg. Chem.*, **45**, 6586 (2006).
[33] I.D. Brown. *Chem. Rev.*, **109**, 6858 (2009).
[34] K. Heussner, M. Grabau, J. Forster, C. Streb. *Eur. J. Inorg. Chem.*, **31**, 5125 (2011).
[35] H. Fu, W.L. Chen, E.B. Wang, J. Liu, S. Chang. *Inorg. Chim. Acta*, **362**, 1412 (2009).
[36] D.W. Yan, L. Zheng, Z.B. Zhang, C.L. Wang, Y. Yuan, D.R. Zhu, Y. Xu. *J. Coord. Chem.*, **63**, 4215 (2010).